

Sea storms hindcast around Calabrian coasts: Seven cases study

S. FEDERICO⁽¹⁾⁽²⁾ and C. BELLECCI⁽¹⁾⁽³⁾

⁽¹⁾ *CRATI Scrl - c/o Università della Calabria - 87036 Rende (CS), Italy*

⁽²⁾ *ISAC-CNR - Via del Fosso del Cavaliere 100, 00133 Roma, Italy*

⁽³⁾ *Dep. STFE, Università degli Studi di Roma "Tor Vergata" - 00133 Roma, Italy*

(ricevuto il 30 Agosto 2004; approvato il 5 Ottobre 2004)

Summary. — The impact of wind field enhanced horizontal resolution on seven sea storms hindcast occurred around Calabrian coasts, the southernmost tip of Italian peninsula, is investigated. Cases studies are simulated by WAM (WAVE Model), a third-generation state-of-the-art wave model. In order to study the effects produced on wave hindcast by surface wind enhanced horizontal resolution, two simulations sets are discussed. The first set uses ECMWF (European Centre for Medium Weather range Forecast) surface wind fields analysis to force WAM model; a second simulations set is produced by forcing WAM model with RAMS (Regional Atmospheric Modeling System) surface wind fields. RAMS simulations use ECMWF analysis as initial and dynamic boundary conditions. Performances are evaluated comparing WAM-modelled wave heights and directions with data at Cetraro and Crotona Wave measuring Buoys (WBs). While wave directions are well reproduced by both simulations sets, *i.e.* using ECMWF or RAMS wind fields to force WAM, differences arise for wave heights. Results show better performances of WAM model when RAMS surface wind field is used. However for two events results are still unsatisfactory using RAMS-modelled wind fields. A possible explanation is given.

PACS 92.60.Gn – Winds and their effects.

PACS 92.10.Hm – Surface waves, tides, and sea level.

PACS 92.10.Fj – Dynamics of the upper ocean.

PACS 92.10.Kp – Sea-air energy exchange processes.

1. – Introduction

The present quality of modelled ocean surface wind fields is generally good. This gives good simulations of waves in open seas. However the situation is different for closed basins [1]. In this case the lack of detailed physiographic features on winds forcing wave models produces a general speed underestimation that has a significant impact on wave modelling. An extensive comparison between modelled wave height using ECMWF wind fields to force WAM and measurements coming from the Italian RON (Rete Ondametrica Nazionale) network shows that wave heights are underestimated by a 30% factor [1,2].

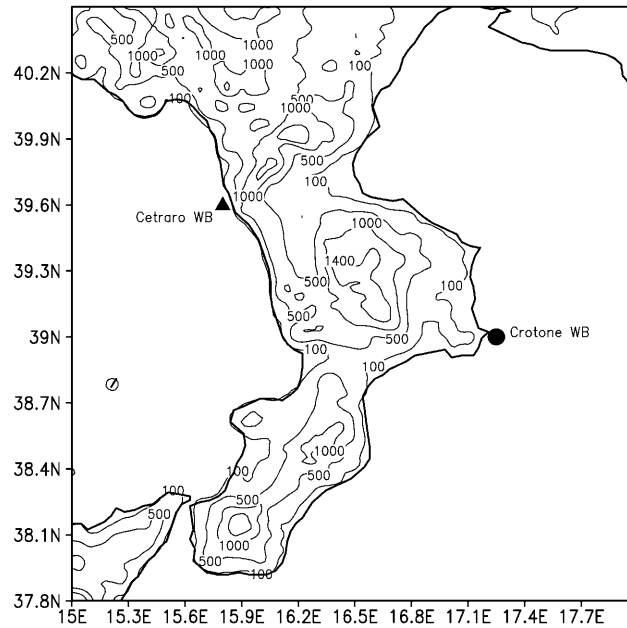


Fig. 1. – Calabria orography averaged over 5 km². WBs positions are also reported.

In this paper we investigate the possibility to improve wave hindcast around Calabrian coasts using surface wind fields produced by a mesoscale model.

Our attention is focused on Calabrian peninsula, the southernmost tip of Italian boot (fig. 1). Calabria ranges between 37°55' and 40° latitude North and between 15°30' and 17°15' longitude East. The western side is bounded by the Tyrrhenian Sea, while the southern and eastern parts are bounded by the Ionian Sea. Apennines run along the peninsula; they are characterized by five main ranges from North to South: Pollino, Catena Costiera, Sila, Serre and Aspromonte. Serre and Catena Costiera peaks heights are about 1500 m while, for others peaks, elevations are about 2000 m.

To assess the impact of RAMS wind field on WAM runs, we compare two simulations sets. The first one uses ECMWF analysis to force WAM model, the second simulations set uses RAMS wind field with 20 km and 5 km horizontal resolution, respectively. Performances assessment is made comparing WAM output and data available at Crotona and Cetraro WBs. These are free-floating WAVEC buoys that record directional wave data. Their locations, in addition to Calabria main topographic features, are reported in fig. 1. Data are available with the same model characteristics, *i.e.* significant wave height, mean wave direction, mean wave period.

Results are preliminary in a statistical sense because they refer to seven sea storms occurred along Calabrian coasts; however simulations are interesting for two different reasons. First of all they give an assessment of the benefits that one should expect during a more extended simulation period; second they present results for severe storms.

Considering the events as a whole we have simulated 28 days and statistics are reported for this period. Table I shows periods selected (excluding spin-up time that, for each simulation, is 12 h). In particular the sea storm occurred in December 1999 is the most intense ever recorded along the Calabrian Tyrrhenian coast. Output from WAM

TABLE I. – *Period selected and days of simulation.*

Sea storm no.	Period selected	Days of simulation
1	17/21 November 1999	4
2	26/30 December 1999	4
3	20/24 January 2000	4
4	25/30 November 2000	5
5	28/31 December 2000	3
6	9/13 January 2004	4
7	20/24 January 2004	4

model is available every three hours, that is the same time interval of WBs.

The paper is organized as follows: next section describes the simulation strategy, then, briefly, we report cases study analyzed. In sect. 4 we give models set-up and resolutions. Results are discussed in sect. 5 and conclusions are given in sect. 6.

2. – Methodology

To study the effects of enhanced horizontal wind field resolution on WAM-modelled waves, two main simulations sets are conducted for each period selected. The first simulation set is made using ECMWF surface wind analysis fields to force WAM model, the second simulation set uses surface wind output from RAMS model, a limited area model (LAM) used at CRATI Srl since 1997. WAM simulations are performed using two nested grids shown in fig. 2. WAM nested-grid boundary conditions are interpolated from first grid output.

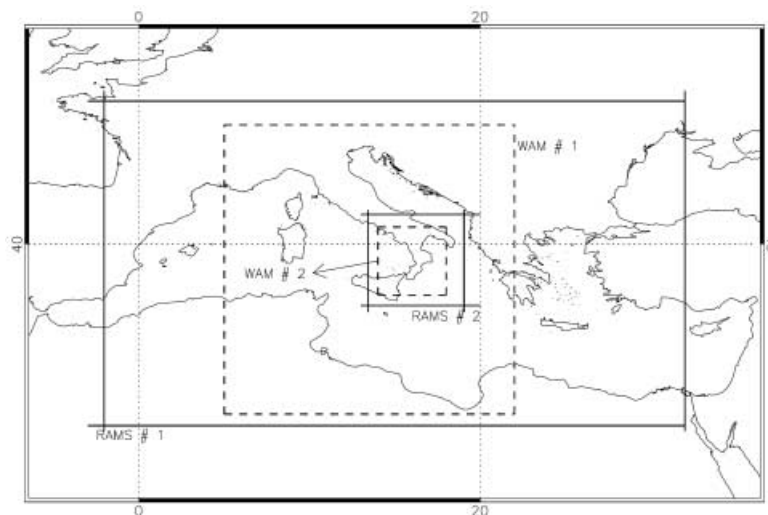


Fig. 2. – Models grids configuration. Solid lines refer to RAMS, dashed lines to WAM. RAMS model uses a two-way interactive grid algorithm; dynamic boundary conditions for the smaller WAM grid (no. 2) are from the largest one (no. 1).

The aim of this study is to give a first assessment to the problem of wave hindcast around Calabrian coasts during severe events, so we use ECMWF analysis as initial and dynamic boundary conditions for LAM simulations. The use of a mesoscale model [3], nested in the ECMWF general circulation model, is useful for two reasons. First the lack of resolution of the latter gives a wind speed underestimation in coastal areas, second the interaction between local orography and atmospheric flow has an impact on storm evolution and, as a consequence, on wind field. This interaction is certainly important for Calabria due to its peculiar geomorphology [4].

So, two main simulations sets are discussed: WAM runs with ECMWF surface wind analysis and WAM runs with RAMS surface wind field. From now on we will refer to the first set as WAM+ECMWF.

In order to better investigate the subject of this paper, two RAMS integrations subsets are considered: the first one has 20 km horizontal resolution and spans the central Mediterranean basin; the second set-up includes a nested grid in RAMS simulations, centred over Calabria, with 5 km grid spacing. We will refer to these simulations as R20 and R5. In both cases simulation duration accounts for 12 h spin-up time. RAMS grids are shown in fig. 2.

The coupling between RAMS and WAM model is one way, *i.e.* RAMS winds are pre-computed and used to force WAM.

In the case of WAM simulations using R20 wind input, RAMS fields are interpolated bilinearly to both WAM grids and reduced to 10 m agl assuming a logarithmic vertical profile. For WAM simulations involving R5 wind field we use the following strategy: R20 wind field is interpolated bilinearly to WAM first grid and R5 wind field is interpolated bilinearly to WAM second grid. Hereafter we will refer to those simulations as WAM+RAMS and WAM+RAMS.5, respectively.

The use of a 5 km wind field is supported by another point of view, in addition to simply enhancing the resolution of coastline geometry. Sea storms are frequently associated with intense precipitation events and Federico *et al.* [5] showed that RAMS rainfall forecast over Calabria was improved by the use of a 6 km grid resolution nested in a coarser 30 km parent grid. Because local winds are influenced by diabatic processes, we report WAM+RAMS.5 results to take into account this issue.

A result found in Mediterranean basin [2] shows that wave significant height has an underestimate of 50% with a variability of 15% on several buoys dislocated in the Adriatic Sea. Remarkably this poor situation is not reflected in wave direction that does not show any substantial bias. As a consequence it is possible to try a statistical procedure by which we look for a suitable wind factor enhancement in order to have better results. In addition, even if computer power is increasing steadily, R5 simulations are expensive in terms of CPU time, so a methodology that uses a statistical approach is helpful. In this paper we adopt the methodology of Cavaleri and Bertotti [2], that we report, shortly, in what follows.

Defining model results with the subscript “mod” we hypothesize the relation between wave height H and wind speed U by the following statement:

$$(1) \quad H_{\text{mod}} \approx (U_{\text{mod}})^{\beta} .$$

Given the measured wave height we have also

$$(2) \quad H_{\text{meas}} \approx (U)^{\beta} .$$

The ratio of (2) to (1) gives

$$(3) \quad \frac{H_{\text{meas}}}{H_{\text{mod}}} = \left(\frac{U}{U_{\text{mod}}} \right)^\beta = \alpha^\beta,$$

where α is the wind enhancement factor. In (3) U and β are unknown quantities. β can be determined, for each buoy, by performing runs with an enhanced wind factor (in our case 2). Indeed, if U' and H' denote the wind speed and the wave height for this “doubling experiment”, we have

$$(4) \quad \beta = \frac{\ln(H'/H_{\text{mod}})}{\ln(U'/U_{\text{mod}})}.$$

In this study we use R20 winds in (1), (3) and (4) instead of ECMWF surface winds as reported in Cavaleri and Bertotti [2].

So we repeated for all the events reported in this paper simulations using doubled R20 wind field to obtain the wind enhancement factor. It turns out to be 1.32 for Cetraro buoy and 1.16 for Crotona buoy. Then we repeated integrations using these enhancement factors for Cetraro and Crotona buoys. Results for this last methodology are preliminary because more cases study must be selected to derive valuable conclusions, *i.e.* to have a better α estimate. With this limitation in mind, we will refer to this integrations set as WAM+RAMS_E (RAMS wind enhanced).

In summary we discuss the following numerical experiments sets:

- 1) WAM_ECMWF, for WAM runs using ECMWF surface wind fields on both WAM grids;
- 2) WAM_RAM5, for WAM runs using R20 surface wind fields on both WAM grids;
- 3) WAM_RAM5.5, for WAM runs using R20 surface wind fields for the first WAM grid and R5 surface wind fields for the second WAM grid;
- 4) WAM_RAM5_E, for WAM runs using R20 enhanced wind fields for both WAM grids.

3. – Cases study

In this section we discuss, briefly, synoptic conditions, derived from ECMWF analysis, that characterized events studied in this paper. Storms choice is based on our data availability and storms features.

Storms main characteristics are reported in table II. “Storm date” column represents the date of maximum wave height record; “buoy” is the buoy where maximum height was measured; “HGT (m)” is the maximum height recorded, in meters, and “WSP (m/s)” is the maximum wind speed, in meters per second, at buoy location. Even if waves are an integrated effect in space and time, last parameter gives a first estimation of storm intensity. It should be emphasized that wind speed is derived from ECMWF analysis and shows the value at the nearest grid point to buoy location.

Among events selected in this study, five had a large impact on the Tyrrhenian coast and two on the Ionian coast. Due to Calabria location and to its climate [6], sea storms are more frequent on the Tyrrhenian side of the peninsula [7]. In addition, sea storms

TABLE II. – *Sea storms main features.*

Storm date	Buoy	HGT (m)	WSP (m/s)
1999-11-19	Cetraro	4.1	7.4
1999-12-28	Cetraro	7.9	10.3
2000-01-23	Cetraro	4.0	8.7
2000-11-27	Cetraro	5.5	10.0
2000-12-30	Cetraro	4.4	7.0
2004-01-11	Crotone	3.4	11.0
2004-01-22	Crotone	4.0	12.0

recorded at Cetraro buoy are seldom recorded at Crotone buoy because if the fetch is large for one buoy it is usually short for the second one.

Storm 1: 1999-11-19

This storm is characterized by a surface low pressure and associated cyclone that developed downwind of the Alps, as often occurs in Italy [8]. Figure 3 shows sea level pressure field at 00Z-20th November, when the sea storm was active at Cetraro buoy. It is clearly visible a low-pressure pattern over the Genova gulf that produced intense winds over the Tyrrhenian Sea. During its evolution this storm crossed Italy from North to South and winds were reinforced by a second cyclone over Balkans (not shown). However,

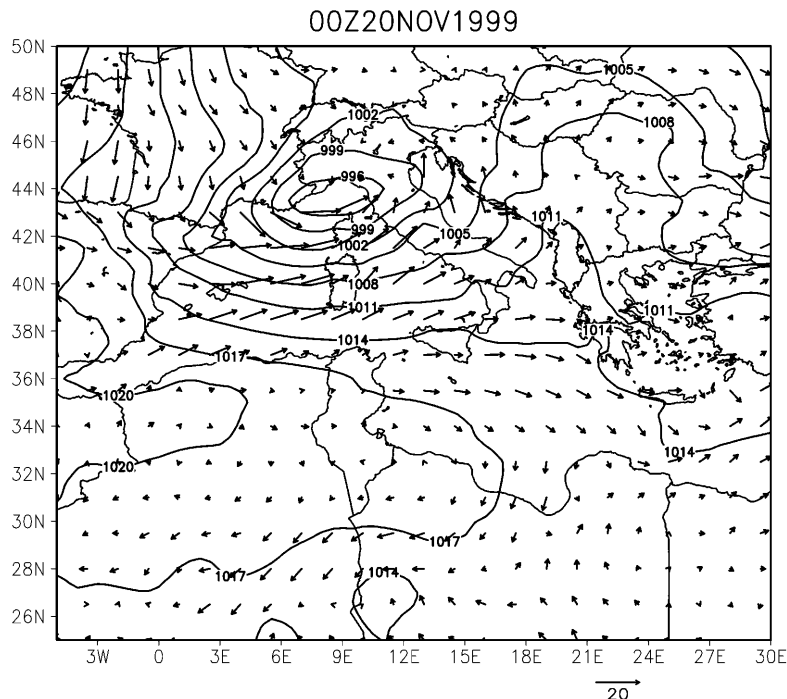


Fig. 3. – Sea level pressure and wind field 10 m agl derived from ECMWF analysis for 20th November 1999 00Z.

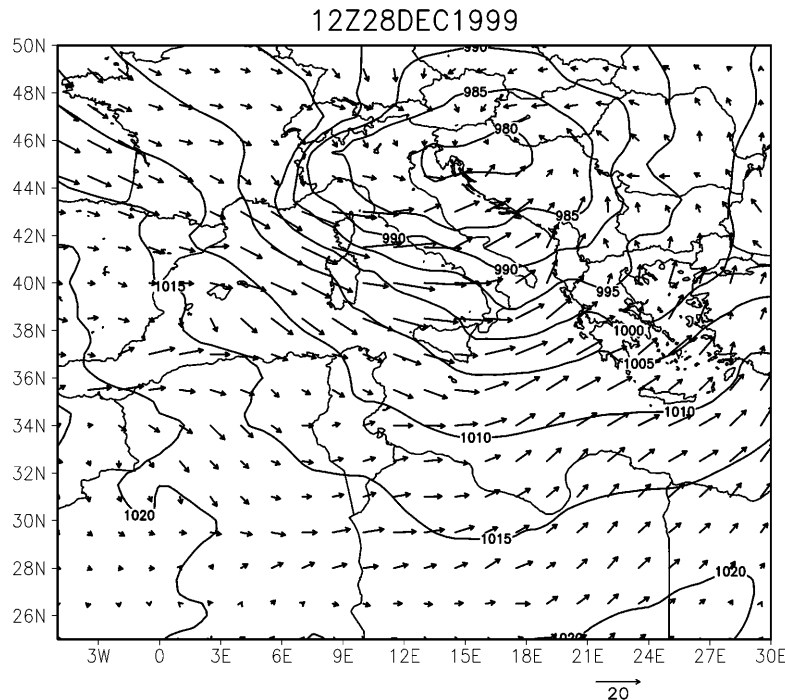


Fig. 4. – As in fig. 3 for 28th December 1999 12Z.

low surface pressure pattern associated with the primary cyclone did not cross Italian peninsula during its evolution and it filled and vanished west of Calabrian coasts.

Storm 2: 1999-12-28

This sea storm is the most intense ever recorded at Cetraro buoy. Maximum wave height was about 8 m and large damages were reported along the Italian Tyrrhenian coast. Large scale was characterized by two different cyclones that developed over North-West Europe and then crossed the country from North-West to South-East. Intense winds developed over the Tyrrhenian Sea. First cyclone produced large wind over the central Mediterranean basin during 27th December while the second storm was active on 29th December. Figure 4 shows surface winds and sea level pressure field derived from ECMWF analysis on 28th December-12Z.

Storm 3: 2000-01-23

This storm was a “typical Tyrrhenian storm” produced by a cyclone (not shown) that generated on the lee side of the Alps and then crossed Italy from North-West to South-East. Wind field for this storm (not shown) was similar to that shown in fig. 4 but wind intensities were lower, as can also be inferred by ECMWF maximum wind speed in correspondence of Cetraro buoy (table II).

Storm 4: 2000-11-27

Also in this case the storm originated on the lee side of the Alps, over the gulf of Genova, however its evolution differed from previous events. Indeed surface low-pressure center moved eastward across northern Italy and reached the Adriatic Sea (18Z-26th

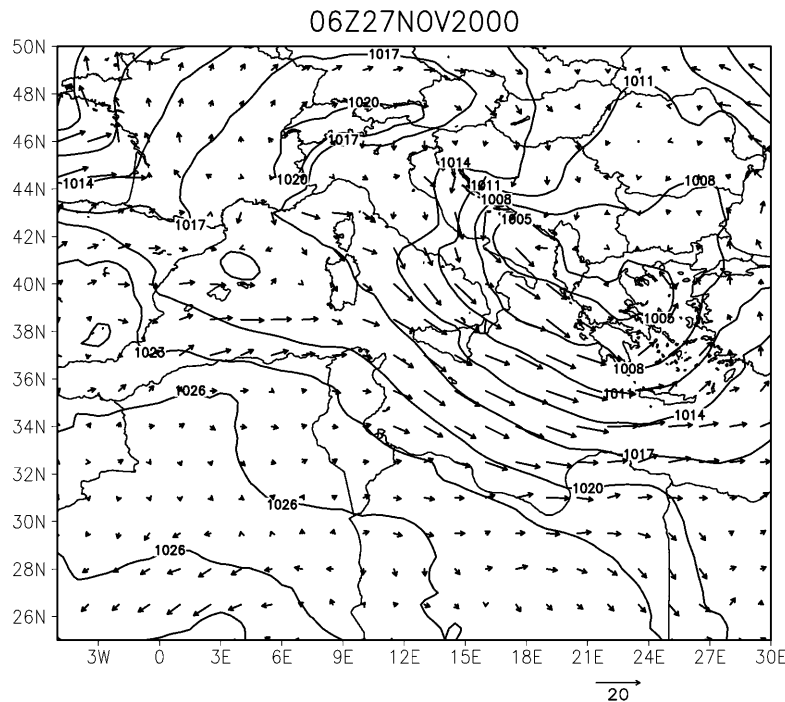


Fig. 5. – As in fig. 3 for 27th November 2000 06Z.

November). Then the storm moved southward and sea level pressure low remained over the Adriatic Sea. Figure 5 shows sea level pressure and surface wind field derived from ECMWF analysis on 27th November-06Z when the sea storm was active at Cetraro buoy. Sea level pressure minimum spreads over Adriatic and Balkans. It is evident that, for Cetraro buoy, fetch for this storm is lower compared to previous events.

Storm 5: 2000-12-30

This storm is somewhat similar to the first three storms presented in this section. In fact, at Cetraro buoy, it was characterized by winds coming mainly from West. However, in this case, the surface pressure low was located further West compared to previous cases and surface winds have a southern component. Figure 6 shows sea level pressure and surface wind fields derived from ECMWF analysis on 30th December-12Z, when the sea storm was active at Cetraro buoy. Comparing fig. 6 with figs. 3, 4 and 5 it is evident that ECMWF winds are lower for 30 December 2000 storm. This behavior is typical during the entire event and is also confirmed by the maximum ECMWF wind speed value (table II)

Storm 6: 2004-01-11

This is the first storm considered that affected noticeably Crotona WB. In its first stage it was characterized by a surface low-pressure pattern that originated on the lee side of the Alps and moved from North-West to South-East across Italy. After, it went over the Adriatic Sea and continued its motion toward Balkans. Figure 7 shows sea level pressure pattern and wind field on 11th January-12Z derived from ECMWF analysis. At this time significant wave heights above 3 m were recorded at Crotona buoy. It is evident

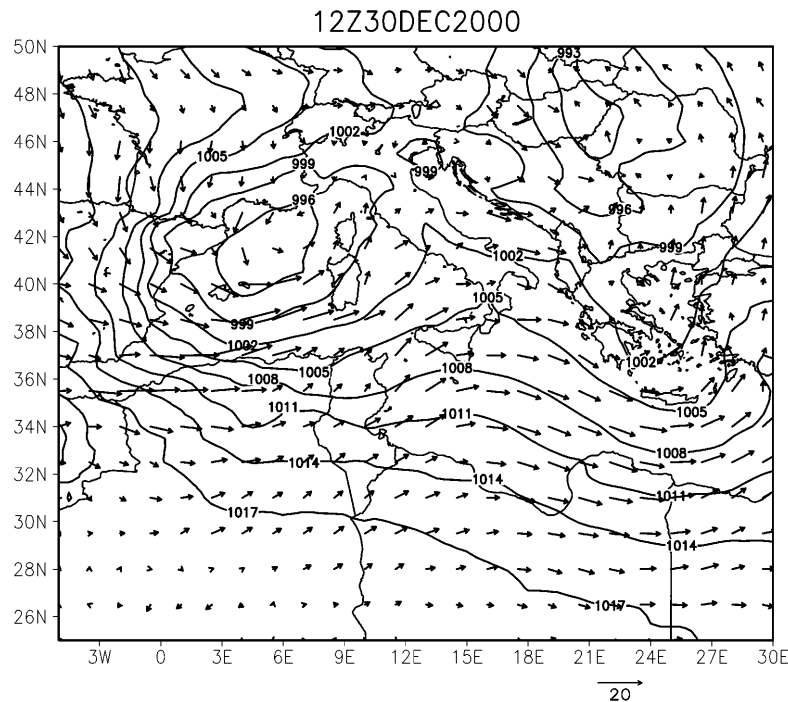


Fig. 6. – As in fig. 3 for 30th December 2000 12Z.

the low-pressure pattern, centered over the Aegean Sea, that produced the storm. Fetch is limited by land (Puglia peninsula) and winds blow quite uniformly over the Calabrian Ionian Sea.

Storm 7: 2004-01-22

This storm was active on the Ionian Sea and affected Crotona buoy. Sea level pressure low (not shown) was located over Greece when the storm fully developed on the eastern Calabrian coast. Wind pattern (not reported) is similar to fig. 7, so fetch was limited by land also for this case study. Maximum wind speed derived from ECMWF analysis in correspondence of Crotona buoy and wave maximum significant height were larger for this storm compared to the previous one.

In summary we can divide cases study considered into this paper into two main groups: the first one is composed of five cases study that affected the Calabrian Tyrrhenian coast; the second group, formed by two cases study, was active on the Ionian side. Even if simulations presented in this paper are not exhaustive of complex cases that occur over Calabria they are helpful to give a first assessment on the subject discussed in this paper and to isolate key factors that can improve wave modeling around this country.

4. – Models

4.1. *RAMS model.* – The following is a brief description of RAMS set-up including options selected. The reader should refer to Pielke *et al.* and Cotton *et al.* [9, 10] for details. Grids configuration is shown in fig. 2. R20 configuration uses the first grid only;

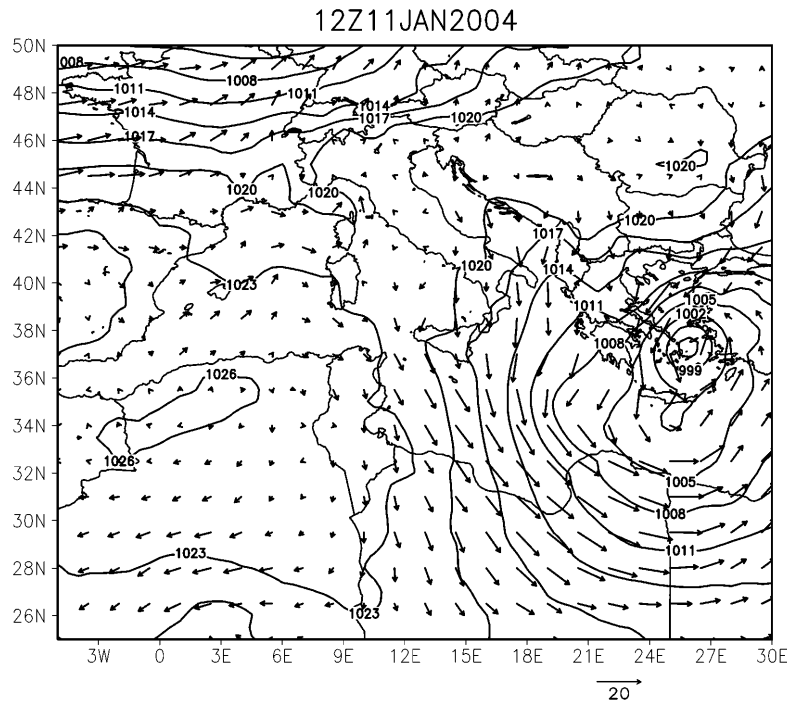


Fig. 7. – As in fig. 3 for 11th January 2004 12Z.

R5 is nested in R20 by a two-way interactive algorithm [11]. Communication from the parent to the nested grid is accomplished immediately following a timestep on the parent grid which updates prognostic fields. The nested-grid timestep is, usually, less than the parent grid time step, so, after the communication, the nested grid is updated in a series of smaller time steps until its integration time equals the parent grid simulation time. At this time, the reverse communication is accomplished.

Thirty levels, up to 15000 m in the terrain following coordinate system, are used in the vertical. Levels are not equally spaced: within the PBL (Planetary Boundary Layer) layers run about 50–200 m thick, while in the middle and upper troposphere they are 1000 m thick. First RAMS level is 20 m above the ground and winds are reduced to 10 m, as requested by WAM, assuming a logarithmic profile.

The parameterization of the surface-atmosphere diabatic processes is described in Walko [12]. Non convective precipitation is calculated from explicit prognostic equations for eight hydrometeors: total water, rain, pristine, cloud particles, ice, snow, hail and aggregates. Convective precipitation is parameterized following Molinari and Corsetti [13] who proposed a simplified form of the Kuo scheme that accounts for updrafts and downdrafts. Sea surface temperature (SST) is a function of the position but, during the simulation, it is held constant in time. The dataset currently used in RAMS contains one degree resolution global monthly climatological SST values.

Initial and dynamic boundary conditions are provided by ECMWF analysis available every 6 hours. The horizontal resolution of the ECMWF analysis is half degree.

4.2. *WAM model.* – In this subsection we give a brief description of WAM configuration used in this paper. For a complete reference the reader should refer to the relevant bibliography [14, 2].

It is assumed that, at a given time t and location (λ, ϕ) the wave condition is represented by the two-dimensional spectrum $F(\lambda, \phi, \theta, f, t)$, where f and ϑ are wave frequency and direction and λ, ϕ are the longitude and latitude, respectively. The evolution of $F(\lambda, \phi, \theta, f, t)$ is described by the wave energy balance equation that, on the spherical earth has the following form:

$$(5) \quad \frac{\partial F}{\partial t} + \frac{1}{\cos \phi} \frac{\partial(\dot{\phi} \cos \phi F)}{\partial \phi} + \frac{\partial(\dot{\lambda} F)}{\partial \lambda} + \frac{\partial(\dot{\vartheta} F)}{\partial \vartheta} = S.$$

In equations reported in this paper dots are time derivatives. S takes into account the physical processes, listed below, while the left-hand side describes the wave energy advection. In addition

$$\begin{cases} \dot{\phi} = v R^{-1} \cos \vartheta, \\ \dot{\lambda} = v \sin \vartheta (R \cos \phi)^{-1}, \\ \dot{\vartheta} = v \sin \vartheta \tan(\phi) R^{-1}, \end{cases}$$

where v is the group velocity and R is the Earth radius.

The source term S can be divided as follows:

$$(6) \quad S = S_{\text{in}} + S_{\text{nl}} + S_{\text{dis}}.$$

In (6) S_{in} is the energy input from the wind field and is parameterized from Miles theory [15]. S_{nl} takes into account non-linear energy transfer between different waves and is parameterized following Hasselmann *et al.* [16].

S_{dis} parameterizes dissipation processes. In deep water the only relevant process is represented by wave breaking [17] while in shallow water other relevant processes are possible, depending on bottom conditions. In our simulations we take into account bottom wave breaking. Parameterization of S can be found in the relevant bibliography.

S_{in} depends on 10 m wind speed through friction velocity u^* ; it is the primary term that changes in our simulations. Obviously, changes in S_{in} affect other terms in (5), however it must be stressed that differences between simulations originate from differences in forcing winds.

WAM model is used in nested configuration (fig. 2). Grid one has 0.1 degree grid spacing in both North-South and West-East directions while grid two spacing is 0.05 degree, in both directions. A discretized spectrum of 25 frequency bands in a logarithmic scale with $\Delta f/f = 0.1$ has been used. Frequency spans from 0.042 Hz to 0.41 Hz. Direction resolution is 30° (12 bands).

5. – Results

In this section we compare modelled and measured values at Crotono and Cetraro WBs. Modelled values are WAM second grid outputs at the nearest grid point to buoy location.

A summary of all simulations is reported in tables III, IV and V for Cetraro buoy (a) and in tables III, IV and V for Crotono buoy (b).

TABLE III. – Mean absolute error (m) for wave height at Cetraro buoy (a) and at Crotona buoy (b). Asterisks are missing data.

a)

MAE–Cetraro (m)	WAM+ECMWF	WAM+RAMS	WAM+RAMS_5	WAM+RAMS_E
1999-11-19	1.36	0.70	<i>0.62</i>	0.63
1999-12-28	2.15	0.80	<i>0.47</i>	0.58
2000-01-23	1.01	0.67	0.54	<i>0.50</i>
2000-11-27	1.30	1.06	<i>0.85</i>	0.93
2000-12-30	1.56	1.37	<i>1.25</i>	1.30
2004-01-11	0.75	0.61	<i>0.54</i>	0.55
2004-01-22	0.54	0.54	<i>0.38</i>	0.46

b)

MAE–Crotona (m)	WAM+ECMWF	WAM+RAMS	WAM+RAMS_5	WAM+RAMS_E
1999-11-19	<i>0.29</i>	0.34	0.31	0.35
1999-12-28	***	***	***	***
2000-01-23	<i>0.30</i>	0.33	0.35	0.33
2000-11-27	<i>0.24</i>	0.54	0.46	0.59
2000-12-30	0.52	0.51	<i>0.45</i>	0.50
2004-01-11	0.61	0.22	<i>0.21</i>	0.26
2004-01-22	0.82	0.52	0.50	<i>0.49</i>

Tables IIIa and IVa report, for each event (row) and for each simulation (column), mean absolute error of significant wave height for Cetraro and Crotona WB, respectively. This error is defined as

$$MAE(m) = \frac{\sum_{i=1}^N |H_{\text{meas}}(i) - H_{\text{mod}}(i)|}{N},$$

where N is the available data number for the simulation considered and depends on case study, as reported in table I, H_{meas} represents the wave height measured and H_{mod} is the corresponding significant wave height simulated. Bold fonts are worst results, italic fonts are best performances.

Since we are investigating severe events another interesting parameter to examine is the error for maximum significant wave height recorded during the event. It is reported in tables IVa and IVb for Cetraro and Crotona WBs, respectively. Rows refer to the event considered and columns refer to the specific simulation. Values reported are $\Delta H = H_{\text{max,meas}} - H_{\text{max,mod}}$ in meters and $|\Delta H/H_{\text{max,meas}}|$ in %. The first value is the difference between the maximum measured wave height and the maximum modelled wave height during the storm. It is positive if models underestimate the wave peak and negative if it overestimates this value. $|\Delta H/H_{\text{max,meas}}|$ is a measure of the absolute relative error for the maximum recorded value. In tables IVa and IVb, bold fonts are worst results, italic fonts are best performances.

Tables Va and Vb report, respectively, mean absolute errors for wave direction at

TABLE IV. – Difference between measured and modelled significant wave height maximum ΔH (m), and absolute relative error $\left| \frac{\Delta H}{H_{\max, \text{meas}}} \right|$ (%) for Cetraro buoy (a) and Crotona buoy (b). Asterisks are missing data.

a)

DATE	WAM+ECMWF		WAM+RAMS		WAM+RAMS_5		WAM+RAMS_E	
	ΔH	$\left \frac{\Delta H}{H_{\max, \text{meas}}} \right $	ΔH	$\left \frac{\Delta H}{H_{\max, \text{meas}}} \right $	ΔH	$\left \frac{\Delta H}{H_{\max, \text{meas}}} \right $	ΔH	$\left \frac{\Delta H}{H_{\max, \text{meas}}} \right $
1999-11-19	1.91	47%	0.64	16%	0.40	10%	<i>0.40</i>	<i>10%</i>
1999-12-28	4.25	53%	1.79	23%	<i>0.65</i>	<i>8%</i>	1.19	15%
2000-01-23	1.40	35%	0.65	16%	0.35	9%	<i>0.21</i>	<i>5%</i>
2000-11-27	3.05	56%	2.56	47%	<i>2.31</i>	<i>42%</i>	2.37	43%
2000-12-30	2.52	57%	2.10	48%	2.01	46%	<i>1.99</i>	<i>45%</i>
2004-01-11	1.24	54%	0.96	42%	0.90	39%	<i>0.90</i>	<i>39%</i>
2004-01-22	0.58	35%	0.75	45%	<i>0.42</i>	<i>25%</i>	0.60	36%

b)

DATE	WAM+ECMWF		WAM+RAMS		WAM+RAMS_5		WAM+RAMS_E	
	ΔH	$\left \frac{\Delta H}{H_{\max, \text{meas}}} \right $	ΔH	$\left \frac{\Delta H}{H_{\max, \text{meas}}} \right $	ΔH	$\left \frac{\Delta H}{H_{\max, \text{meas}}} \right $	ΔH	$\left \frac{\Delta H}{H_{\max, \text{meas}}} \right $
1999-11-19	<i>0.005</i>	<i>0.4%</i>	-0.5	34%	-0.4	30%	-0.7	47%
1999-12-28	***	***	***	***	***	***	***	***
2000-01-23	0.4	23%	<i>0.10</i>	<i>6%</i>	16%	0.1	0.1	6%
2000-11-27	<i>-0.02</i>	<i>0.1%</i>	-0.8	36%	-0.7	31%	-0.9	44%
2000-12-30	<i>0.4</i>	<i>24%</i>	0.6	33%	0.74	41%	0.59	32%
2004-01-11	1.1	33%	<i>-0.05</i>	<i>1%</i>	-0.24	7%	-0.26	8%
2004-01-22	1.3	32%	0.64	16%	0.5	13%	<i>0.5</i>	<i>12%</i>

Cetraro and Crotona buoys. This error is defined as

$$DMAE(^{\circ}) = \frac{\sum_{i=1}^N |WAVE_DIR_{\text{meas}}(i) - WAVE_DIR_{\text{mod}}(i)|}{N},$$

where N is the available data number for the simulation considered, $WAVE_DIR_{\text{meas}}$ is wave direction measured and $WAVE_DIR_{\text{mod}}$ is the paired wave direction simulated. In this paper this parameter is the direction where waves are going computed clockwise from North and values are in degrees. In tables Va and Vb bold fonts are worst results and italic fonts are best performances.

Before single-event discussion it is interesting to give a general assessment of tables III, IV and V.

First of all we note that storms occurred in 1999 and 2000 were recorded at Cetraro buoy and those occurred in 2004 were at Crotona buoy. So results for table IIIa are particularly interesting up to 2004 storms. Considering these cases it is evident that the worst results are always obtained for WAM+ECMWF simulations. Stated in other terms the use of RAMS surface wind field has a large impact on the wave height mean error at Cetraro buoy. Best performances are obtained for WAM+RAMS_5 simu-

TABLE V. – Mean absolute error ($^{\circ}$) for wave direction at Cetraro buoy (a) and Crotona buoy (b). Asterisks are missing data.

a)

DMAE–Cetraro ($^{\circ}$)	WAM+ECMWF	WAM+RAMS	WAM+RAMS.5	WAM+RAMS.E
1999-11-19	9	10	10	11
1999-12-28	9	8	8	7
2000-01-23	9	9	9	8
2000-11-27	7	8	8	9
2000-12-30	6	4	6	6
2004-01-11	17	14	17	16
2004-01-22	11	6	10	9

a)

DMAE–Crotona ($^{\circ}$)	WAM+ECMWF	WAM+RAMS	WAM+RAMS.5	WAM+RAMS.E
1999-11-19	29	22	30	29
1999-12-28	***	***	***	***
2000-01-23	65	58	69	65
2000-11-27	28	27	29	31
2000-12-30	34	30	31	40
2004-01-11	25	29	26	21
2004-01-22	22	24	22	22

lations, *i.e.* using the 5 km resolution wind field simulated by RAMS. WAM+RAMS.E has the best performance for the 2000-01-23 case. WAM+RAMS.5 always outperforms WAM+RAMS.

A deeper examination of table IIIa, however, highlights that mean absolute error reduction from ECMWF winds to R20 winds is greater than the reduction from R20 to R5 wind fields. In addition for two events, *i.e.* 2000-11-27 and particularly for 2000-12-30, improvements due to enhanced wind resolutions are small and results unsatisfactory.

Considering wave height mean absolute error at Crotona buoy, table IIIb, there is particular interest in the last two rows because they refer to sea storms. The effect of enhanced resolution produces a sizeable reduction of mean absolute wave height error. Large error reduction is mainly obtained using R20 wind fields compared to ECMWF analysis and there is only a minor reduction using R5 wind field.

For “less interesting cases” that did not occur at the buoy considered, *i.e.* the last two rows of table IIIa and the first five rows of table IIIb, simulations outputs are controversial. Results using enhanced horizontal resolution do not always outperform WAM+ECMWF.

Table IVa reports errors for maximum height modelled and measured at Cetraro buoy. The first five rows are sea storms recorded at this WB. For all these events the worst performances are for WAM+ECMWF. ΔH is always positive, *i.e.* simulated maximum wave heights always underestimate measurements. If we exclude the 2000-01-23 case, the error is about 50% of maximum recorded values for WAM+ECMWF. It follows that the maximum wave height modelled for this simulations set is about 50% of the maximum recorded value. Error for 1999-12-28 is remarkably high (4.25 m). Maximum wave height hindcast is improved using the enhanced wind resolution for all

cases. Considering WAM+RAMS there is a large error reduction for the first three events while minor improvements are obtained for 2000-11-27 and 2000-12-30 cases even if there is a 10% relative error reduction. Best performances are for R5 wind fields in two cases and for WAM+RAMS_E in three cases.

Considering table IVb for Crotona buoy, the last two rows, that are the most representative, show a sensible reduction of the maximum wave height error using enhanced resolution wind fields to force WAM model. This confirms the improvements obtained by the methodology proposed in this paper for waves hindcast around Calabrian coasts.

For 2004-01-22 case results are similar for WAM_RAMS_5 and WAM_RAMS_E that has best performances, while for 2004-01-11 best results are for WAM+RAMS. Wave heights modelled at Crotona buoy are sometimes overestimated by simulations. In particular performance degradation of WAM+RAMS_5 and WAM+RAMS_E compared to WAM+RAMS for 2004-01-11 case are due to an overestimation of the maximum significant wave height.

For less interesting cases, WAM+ECMWF performances are comparable with those obtained by wind enhanced resolution simulations.

Table Va shows the mean absolute error for the wave direction at Cetraro buoy. Two main results are evident: a) performances are good for all storms considered; b) performances are equivalent for different models configurations. Table Vb shows the mean absolute error for the wave direction simulated at Crotona buoy. Errors are similar for different simulations sets. For Crotona buoy, however, errors are larger compared to Cetraro WB. Due to its geographical location, Crotona buoy is characterized by lower wave heights and phenomena are often associated to local scales. This determines a greater variability of the wave direction and lower performances. This is confirmed by the last two rows of table Vb associated with severe events. In these cases large-scale forcing is more intense and errors decrease.

After these general considerations, we turn to single-event analysis.

Storm 1: 1999-11-19

Figure 8a shows the comparison between buoy data, WAM+ECMWF and WAM+RAMS models for Cetraro buoy. There are two main peaks partially reproduced by WAM simulations. For this storm wind resolution enhancement has a large impact on wave simulation and the mean absolute error is halved. However, also using R20 wind fields there is a general underestimation of the wave height. Figure 8b shows the comparison between buoy data, WAM+RAMS_5 and WAM+RAMS_E. Compared to fig. 8a there is an enhancement of the second wave peak. Figure 8b results are comparable for both WAM configurations, however WAM_RAMS_5 better reproduces storm evolution between maxima. Improvement of WAM results, using LAM wind fields compared to ECMWF data, is not only related to a more detailed coastline representation but also to the larger precipitation amounts simulated. For this case, R5 simulation produces more than 120 mm rainfall over Catena Costiera and more than 150 mm over Pollino and the influence of mesoscale features on local wind evolution was considerable. For R20 model simulation the precipitation maximum over Pollino is 65 mm and rainfall maximum over Catena Costiera is 30 mm. Raingauge data are not available to us to confirm this hypothesis, however it is important to note that precipitation has a sizeable impact on local winds and, as a consequence, on waves.

Figure 8c reports the wave direction measured at Cetraro buoy for WAM+RAMS_5 and WAM+RAMS_E models set-up. Both simulations are able to well represent storm evolution. WAM+RAMS_E is the worst result for this case study (table Va) and it

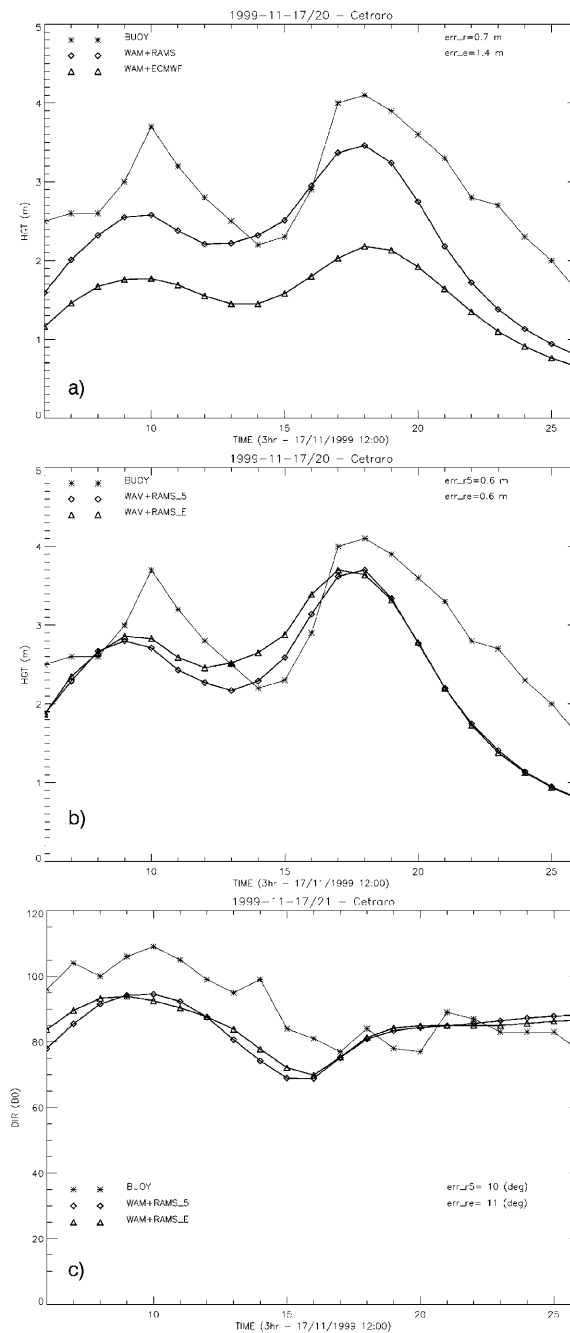


Fig. 8. – a) Comparison between wave heights measurements, WAM+ECMWF and WAM+RAMS modelled field for Cetraro buoy. Results are shown every 3 h. Simulation starts at 12Z 17th November 1999. Asterisks refer to buoy data, triangles to WAM+ECMWF, diamonds to WAM+RAMS. Data are plotted only for the most intense part of the sea storm. Mean absolute errors are also reported. b) As in a) but for WAM+RAMS_5 and WAM+RAMS_E. Measurements are reported for comparison. Asterisks refer to buoy data, triangles to WAM+RAMS_E, diamonds to WAM+RAMS_5. c) As in b) but for wave directions.

follows that directions are well represented by all models configurations.

Storm 2: 1999-12-28

Figure 9a shows the comparison between measurements and model outputs for WAM + ECMWF and WAM+RAMS configurations. There is a large impact of LAM winds on WAM simulations. Indeed the mean absolute error decreases from 2.15 m for WAM + ECMWF to 0.80 m for WAM+RAMS configuration. In addition mean absolute difference between measured and simulated wave height maximum decreases from 4.25 m in WAM+ECMWF case to 1.79 m in WAM+RAMS. R5 wind field gives best performances. Results for this configuration and for WAM+RAMS_E are shown in fig. 9b. WAM+RAMS_5 absolute maximum wave height error is 0.65 m (8%). A sizeable improvement is also obtained using R5 compared to R20 wind fields, mainly in the representation of wave maximum. Also this case study was characterized by large precipitation amounts simulated over mountains peaks. In particular, precipitation for R5 simulation was more than 100 mm over Pollino peak and about 50 mm in the northern part of Catena Costiera. These values are roughly halved in R20 simulation.

Wave directions (not shown) are well represented by all configurations and are not discussed further.

Storm 3: 2000-01-23

Figure 10a shows wave heights simulated by WAM_ECMWF and WAM_RAM_S configurations. Also for this case there is a large impact of RAMS wind fields on WAM simulations. Wave height errors are reduced in absolute mean value and maximum value. Better performances are obtained using statistically enhanced resolution and R5 wind fields (fig. 10b). Wave directions (not shown) are well represented by all models configurations.

Storm 4: 2000-11-27

Figure 11a reports wave heights measured and simulated by WAM+ECMWF and WAM+RAMS at Cetraro buoy. Even if there is an improvement using enhanced wind horizontal resolution, measurements are not well represented. A reduction of modelled errors is obtained using R5 wind field, mainly during the first stage of the sea storm. However errors are large for all simulations and the main part of the event is missed.

Wave directions (not shown) are well simulated by all models and reflect the presence of a well-defined large-scale forcing.

Wind speeds intensities from ECMWF are comparable with other events studied in this paper, for which wave heights are larger than those reported in figs. 11a and b.

Figure 11c shows wind fields, derived from ECMWF analysis, at 06Z and 18Z-27th November, when the sea storm was active at Cetraro buoy. Large arrows heads refer to 18Z. There is a sizeable component from North. In addition, during storm evolution, winds rotate southerly, as shown in fig. 11c, and acquire a more intense component from North. Due to the presence of land, it follows that, for this event, fetch is limited compared to previous events. Using a more general approach, Cavaleri and Bertotti [1] showed that ECMWF modelled wind fields bias increases for decreasing fetches. This bias is transferred to RAMS simulations that are not able, for this case, to correct wind fields. We note also that, among all events simulated at Cetraro buoy, this one is associated with the lowest simulated rain amounts over mountain peaks around Cetraro buoy (less than 40 mm for R5 simulation) and local circulation is only partially affected by humid processes.

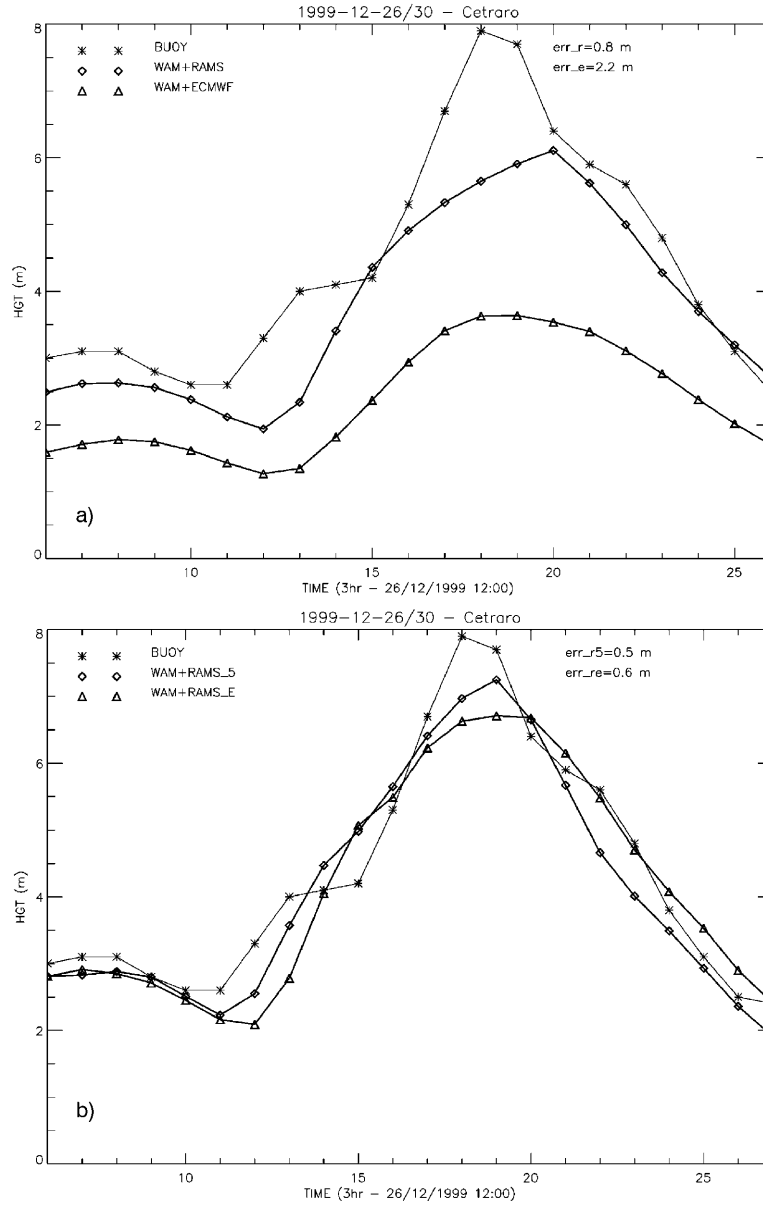


Fig. 9. - a) Comparison between wave heights measurements, WAM+ECMWF and WAM+RAMS modelled field for Cetraro buoy. Results are shown every 3 h. Simulation starts at 12Z 26th December 1999. Asterisks refer to buoy data, triangles to WAM+ECMWF, diamonds to WAM+RAMS. Data are plotted only for the most intense part of the sea storm. Mean absolute errors are also reported. b) As in a) but for WAM+RAMS_5 and WAM+RAMS_E. Measurements are reported for comparison. Asterisks refer to buoy data, triangles to WAM+RAMS_E diamonds to WAM+RAMS_5.

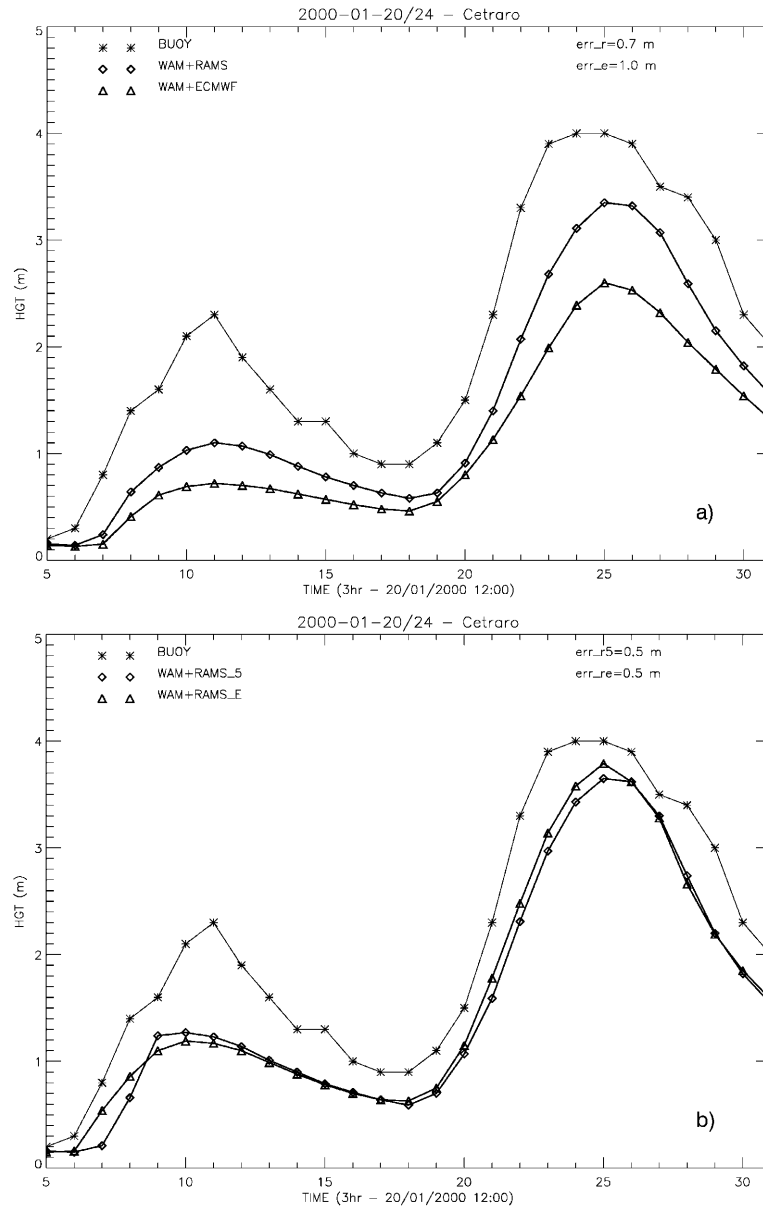


Fig. 10. - a) Comparison between wave heights measurements, WAM+ECMWF and WAM+RAMS modelled values for Cetraro buoy. Results are shown every 3 h. Simulation starts at 12Z 20th January 2000. Asterisks refer to buoy data, triangles to WAM+ECMWF, diamonds to WAM+RAMS. Data are plotted only for the most intense part of the sea storm. Mean absolute errors are also reported. b) As in a) but for WAM+RAMS₅ and WAM+RAMS_E. Measurements are reported for comparison. Asterisks refer to buoy data, triangles to WAM+RAMS_E, diamonds to WAM+RAMS₅.

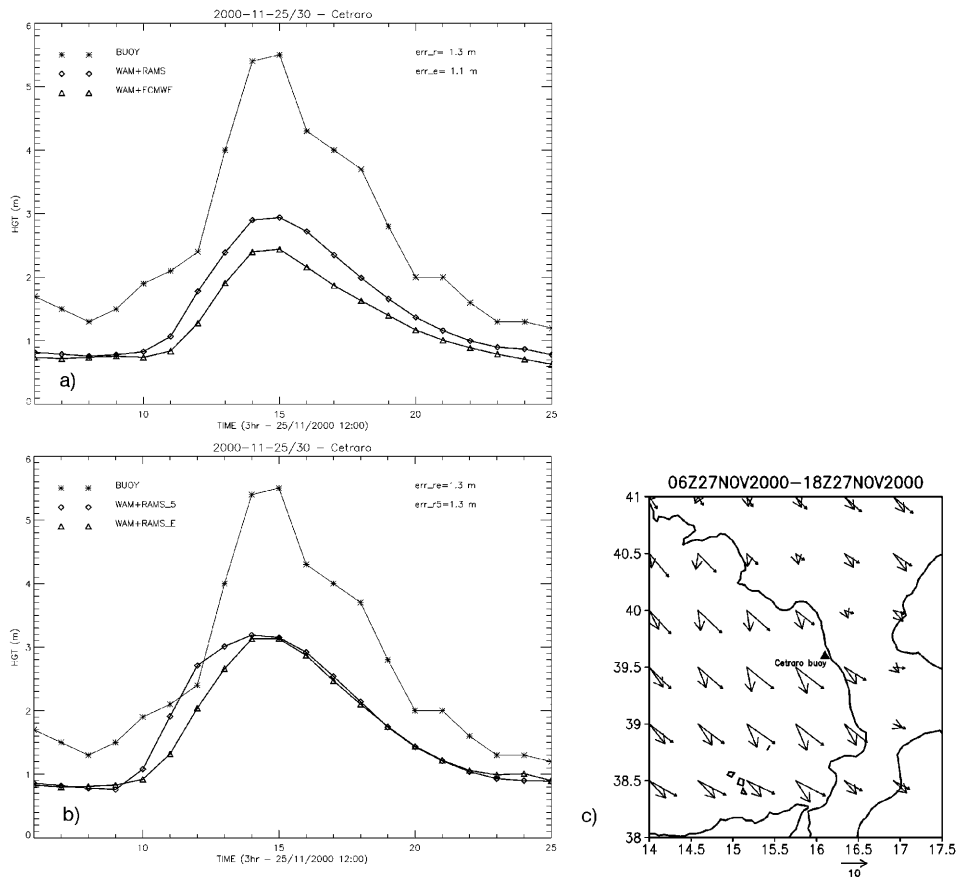


Fig. 11. - a) Comparison between wave heights measurements, WAM+ECMWF and WAM+RAMS modelled values for Cetraro buoy. Results are shown every 3 h. Simulation starts at 12Z 25th November 2000. Asterisks refer to buoy data, triangles to WAM+ECMWF, diamonds to WAM+RAMS. Data are plotted only for the most intense part of the sea storm. Mean absolute errors are also reported. b) As in a) but for WAM+RAMS_5 and WAM+RAMS_E. Measurements are reported for comparison. Asterisks refer to buoy data, triangles to WAM+RAMS_E, diamonds to WAM+RAMS_5. c) Wind fields derived from ECMWF analysis at 06Z and 18:00 Z 27th November. Larger arrows heads refer to 18Z.

Storm 5: 2000-12-30

Figure 12 shows results for WAM+ECMWF and WAM+RAMS simulations compared to Cetraro buoy measurements. Improvements of enhanced wind resolution are minor and results unsatisfactory. Same consideration applies for R5 wind fields and RAMS enhanced wind simulations. On the contrary, as often happens in modeling waves in closed basins [1, 2], wave directions are well simulated by all models configurations and reflect the presence of a well-defined direction in large-scale forcing.

For this case, simulations errors arise, likely, from large-scale forcing that is not properly represented by ECMWF analysis. As noticed in sect. 3 sea level pressure gradients and surface wind speeds are lower for this sea storm compared to November 1999 case study. However, the wave height at Cetraro buoy measured during this storm is larger

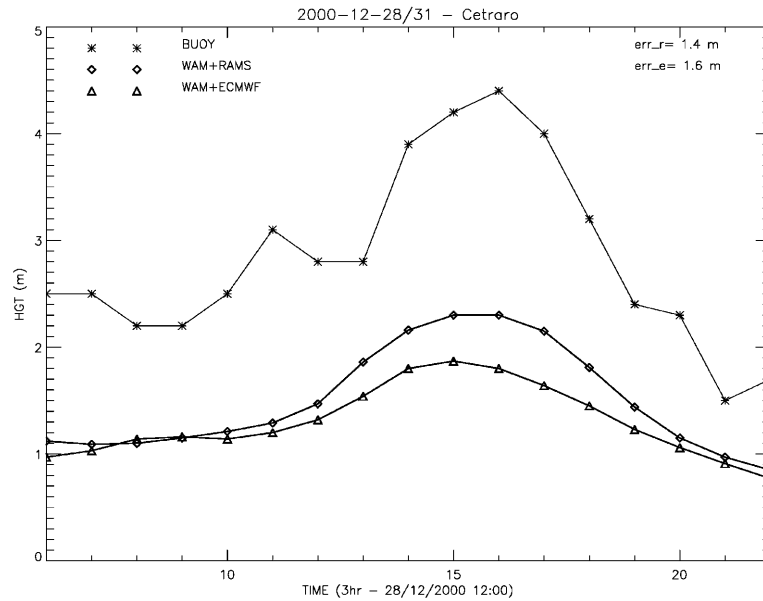


Fig. 12. – Comparison between wave heights measurements, WAM+ECMWF and WAM+RAMS modelled values for Cetraro buoy. Results are shown every 3 h. Simulation starts at 12Z 28th December 2000. Asterisks refer to buoy data, triangles to WAM+ECMWF, diamonds to WAM+RAMS. Data are plotted only for the most intense part of the sea storm. Mean absolute errors are also reported.

compared to the 1999 event. To better verify this point, we analyzed all wind fields of these two storms in the area from 12°E to 16°E and from 38°N to 42°N. This area individuates roughly the southern part of the Tyrrhenian basin. Surface wind speed average over the southern Tyrrhenian sea was always lower than November 1999 case study. At the time when the maximum wave height was recorded at Cetraro buoy, surface wind speed average over the area introduced above for December 2000 sea storm is about 7 m/s while for November 1999 case study it is 12 m/s. This behavior is confirmed during the entire simulation time.

Storm 6: 2004-01-11

This is the first case simulated in this paper that affected Crotona buoy. Figure 13a shows results for WAM+ECMWF and WAM+RAMS simulations. There is a sizeable improvement using RAMS wind fields instead of ECMWF analysis. Errors reduction is large in both the mean absolute value and the maximum wave height. Figure 13b shows results for WAM+RAMS.5 and WAM+RAMS.E simulations. Both configurations overestimate the maximum height, however they are able to better follow the sea storm time evolution, particularly the WAM+RAMS.5. This is another remarkable result found in this work. R5 simulations give a better representation of the storm evolution even when wave simulation is well reproduced by R20 wind fields.

Figure 13c shows the comparison between wave directions measured for Crotona buoy and modelled by WAM+ECMWF and WAM+RAMS configurations. There is greater variability of this parameter at Crotona buoy compared to Cetraro as can be inferred from figs. 13c and 8c. This result is valid for all cases study modelled in this paper. Wave

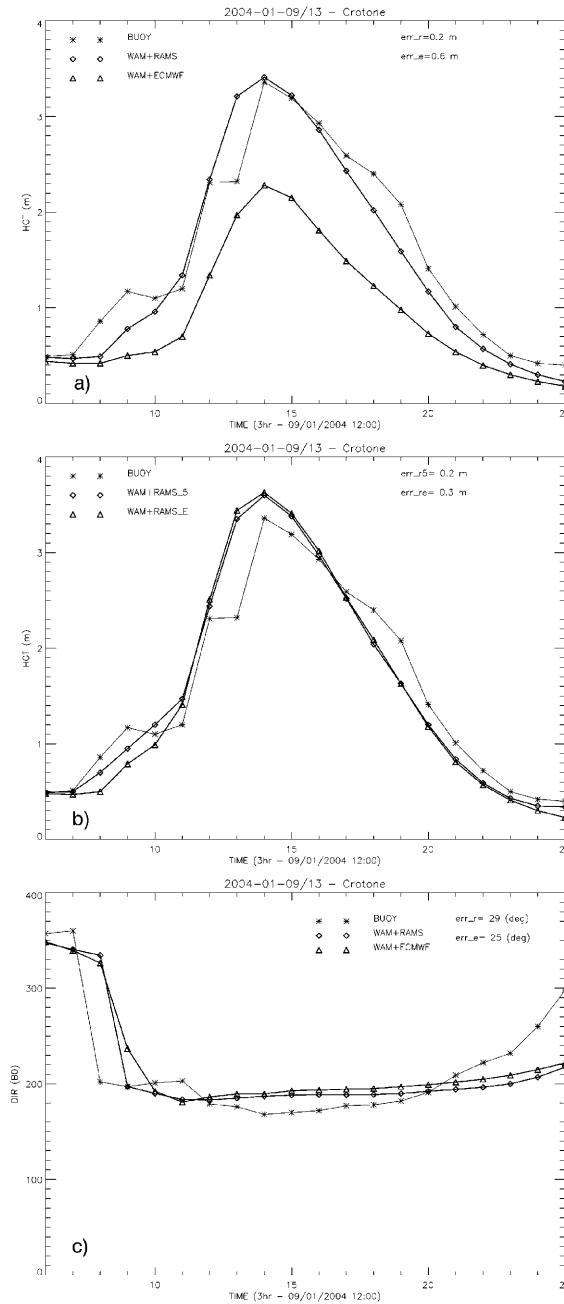


Fig. 13. - a) Comparison between wave heights measurements, WAM+ECMWF and WAM+RAMS modelled values for Crotona buoy. Results are shown every 3 h. Simulation starts at 12Z 09th January 2004. Asterisks refer to buoy data, triangles to WAM+ECMWF, diamonds to WAM+RAMS. Data are plotted only for the most intense part of the sea storm. Mean absolute errors are also reported. b) As in a) but for WAM+RAMS_5 and WAM+RAMS_E. Measurements are reported for comparison. Asterisks refer to buoy data, triangles to WAM+RAMS_E diamonds to WAM+RAMS_5. c) As in a) but for wave directions.

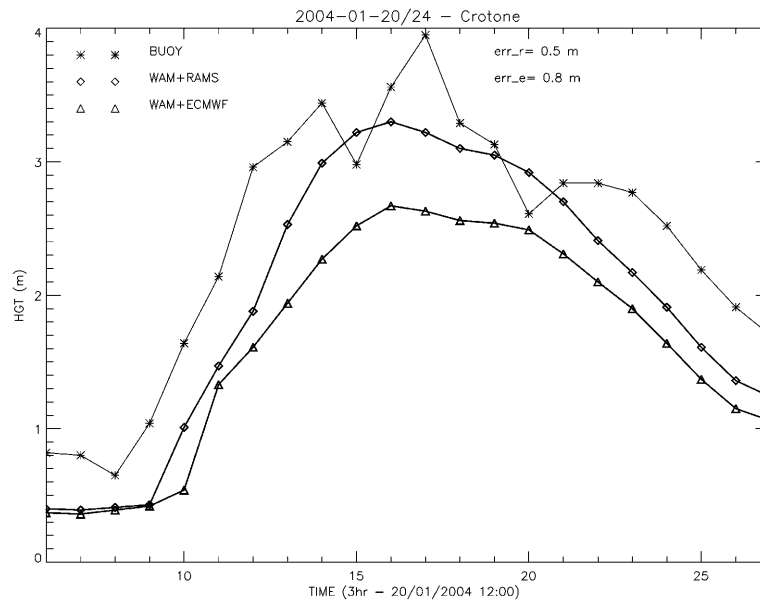


Fig. 14. – Comparison between wave heights measurements, WAM+ECMWF and WAM+RAMS modelled values for Crotona buoy. Results are shown every 3 h. Simulation starts at 12Z 20th January 2004. Asterisks refer to buoy data, triangles to WAM+ECMWF, diamonds to WAM+RAMS. Data are plotted only for the most intense part of the sea storm. Mean absolute errors are also reported.

direction changes at Crotona buoy, in addition, are associated with low wave heights, as shown by figs. 13a and 13c, when there is no clear large-scale forcing. These situations are more difficult to simulate. A better evaluation of local wind through data assimilation should improve results for these cases.

Storm 7: 2004-01-22

For this storm results are similar to the previous one and similar considerations apply. Large differences are found comparing WAM_ECMWF and WAM_RAMs models as shown in fig. 14. Similar results are obtained for WAM_RAMs, WAM_RAMs.5 and WAM_RAMs.E. Wave direction is well simulated by all model configurations.

It is interesting to note that for both Crotona sea storms, precipitation simulated by R5 and R20 configurations is negligible. This helps to explain small differences between WAM+RAMS and WAM+RAMS.5 results.

6. – Conclusions

In this paper we give a first assessment of the effects produced by wind field horizontal resolution enhancement, compared to ECMWF analysis, on wave hindcast around Calabrian coasts. A total of 28 days are simulated and statistics are reported for this period. Even if simulations cannot be exhaustive of all complex sea storms that occur around Calabrian coasts, few conclusions can be derived from this work.

- 1) There is a large impact of R20 wind fields on simulated sea storms. Configuration that uses R20 wind fields performs always better than ECMWF analysis. When

large-scale forcing is well represented in the general circulation model, the maximum wave height and the mean absolute errors are more than halved. When large-scale forcing is not well represented in ECMWF analysis, improvements are smaller and results unsatisfactory even using R5 wind fields.

- 2) Considering all simulations, the best results are obtained for R5 wind field. Improvements are more relevant when two conditions are met: a) large-scale forcing is represented properly in ECMWF analysis; b) simulated rainfall in the area interested by the storm is not negligible.
- 3) Differences between WAM+RAMS_5 and WAM+RAMS_E are usually negligible. The use of R5 is recommended from a physical point of view, while the second technique is preferable from a computational point of view. It should be stressed that our simulations are conducted considering sea storms and this is the best condition for WAM+RAMS_E. We expect lower performances when applied to more general cases.
- 4) Wave direction is well simulated for all models configurations. When large-scale forcing is not intense errors increase.
- 5) Considering calm sea conditions there is no significant improvement using RAMS winds instead of ECMWF analysis.

Last two points could be improved by data assimilation technique and simulations are underway to better assess this subject.

* * *

This work was partially funded by “Ministero dell’Università e della Ricerca Scientifica” in the framework of the project “Sviluppo di Distretti Industriali per le Osservazioni della Terra”. We thank Dott. R. PURINI who provided thoughtful and constructive comments and suggestions.

REFERENCES

- [1] CAVALERI L. and BERTOTTI L., *Tellus A*, **56** (2004) 167.
- [2] CAVALERI L. and BERTOTTI L., *Mon. Weather Rev.*, **125** (1997) 1964.
- [3] PIELKE R. A., *Mesoscale Meteorological Modelling* (Academic Press) 2002.
- [4] FEDERICO S., BELLECCI C. and COLACINO M., *Nuovo Cimento C*, **26** (2003) 7.
- [5] FEDERICO S., AVOLIO E., BELLECCI C. and COLACINO M., *Nuovo Cimento C*, **26** (2003) 663.
- [6] COLACINO M., CONTE M. and PIERVITALI E., *Elementi di climatologia della Calabria*, IFA-CNR (1997).
- [7] FRANCO L. and CONTINI P., *PIANC Bull.*, **94** (1997) 536.
- [8] BUZZI A. and TIBALDI S., *Q. J. R. Meteorol. Soc.*, **104** (1978) 271.
- [9] PIELKE R. A., COTTON W. R., WALKO R. L., TREMBACK C. J., LYONS W. A., GRASSO L. D., NICHOLLS M. E., MURRAN M. D., WESLEY D. A., LEE T. H. and COPELAND J. H., *Meteorol. Atmos. Phys.*, **49** (1992) 69.
- [10] COTTON W. R., PIELKE R. A. SR., WALKO R. L., LISTON G. E., TREMBACK C. J., JIANG H., MCANELLY R. L., HARRINGTON J. Y., NICHOLLS M. E., CARRIO G. G., MCFADDEN J. P., *Meteorol. Atmos. Phys.*, **82** (2003) 5.
- [11] WALKO R. L., TREMBACK C. J., PIELKE R. A. and COTTON W. R., *J. Appl. Meteorol.*, **34** (1994) 994.

- [12] WALKO R. L., BAND L. E., BARON J., KITTEL T. G., LAMMERS R., LEE T. J., OJIMA D., PIELKE R.A. SR., TAYLOR C., TAGUE C., TREMBACK C. J. and VIDALE P. L., *J. Appl. Meteorol.*, **39** (2000) 931.
- [13] MOLINARI J. and CORSETTI T., *Mon. Weather Rev.*, **113** (1985) 485.
- [14] The WAMDI-Group, *J. Phys. Oceanogr.*, **18** (1988) 1775.
- [15] MILES J. W., *J. Fluid Mech.*, **3** (1957) 185.
- [16] HASSELMANN S., HASSELMAN K., ALLENDER J. H. and BARNER T. P., *J. Phys. Oceanogr.*, **15** (1985) 1378.
- [17] KOMEN G. J., HASSELMANN S. and HASSELMAN K., *J. Phys. Oceanogr.*, **14** (1984) 1271.